Direct observation of ferrimagnetic ordering in inverse Heusler alloy Mn_2CoAl

Zhendong Chen[1, #], Wenqing Liu[1, 2, #], Peng Chen[3], Xuezhong Ruan[1*], Jiabao Sun[2], Ruobai Liu[4], Cunxu Gao[3], Jun Du[4], Bo Liu[5*], Hao Meng[5], Rong Zhang[1], and Yongbing Xu[1,6*]

1. Jiangsu Provincial Key Laboratory of Advanced Photonic and Electronic Materials, School of Electronic Science and Engineering, Nanjing University, Nanjing 210093, China.
2. Department of Electronic Engineering, Royal Holloway University of London Egham, Surrey TW20 0EX, United Kingdom.
3. Key Laboratory for Magnetism and Magnetic Materials of the Ministry of Education, Lanzhou University, Lanzhou 730000, China.
4. National Laboratory of Solid State Microstructures and Department of Physics, Nanjing University, Nanjing 210093, China
5. Key Laboratory of Spintronics Materials, Devices and Systems of Zhejiang Province, Lixin road, Linan, Hangzhou 311300, China
6. York-Nanjing Joint Centre (YNJC) for Spintronics and Nano Engineering, Department of Electronics, The University of York, York YO10 5DD, UK.

[#] These authors contributed equally to this work.

* The corresponding authors. E-mail: xzruan@nju.edu.cn; liubo@hikstor.com; ybxu@nju.edu.cn.

Abstract:

The compensated ferrimagnetic Heusler compounds with high spin polarization and low net magnetic moment are strategically important materials for spin-logic and further energy-efficient spintronic applications. However, the element-resolved magnetic ordering of these compensated ferrimagnets remains an open issue. Here we report a direct observation of the spin and orbital moments of the B2 phase Mn_2CoAl thin film using the synchrotron-based X-ray magnetic circular dichroism (XMCD) technique. An ferrimagnetic ordering between Mn and Co elements and a compensated-ferrimagnet-like small net magnetic moment of only 0.34 μ_B/f.u. was observed unambiguously in the B2 Mn_2CoAl. The antiparallel coupling between Mn and Co is attributed to the mixture of the Mn(B) and Al occupation in the B2 phase Mn_2CoAl lattice. This work demonstrates the great potentials of the compensated ferrimagnetic half metallic inverse Heusler compounds Mn_2CoAl for spintronic applications.

Heusler compounds with their half-metallicity nature are capable of providing 100 % spin polarization at the Fermi Level, which makes them an ideal source for spin current in various spintronic devices[1-7]. Among the Heusler compounds, the unique compensated ferrimagnetism has been found in some Heusler compounds, for example Mn_2Ru_xGa and $Mn_{2-x}Pt_xGa$[8-12]. In such materials, the moments of magnetic atoms are arranged as antiparallel ordering with different moment magnitudes, while the total net magnetization is predicted to be zero or very low due to the complete compensation of all the atomic moments with opposite orientations. The compensated ferrimagnets exhibit zero or low stray field and robustness of magnetic moment arrangement in external field, promising extensive potential applications in spintronic devices[8][11]. In recent years, a new kind of inverse Heusler compounds with a $CuHg_2Ti$-type structure (XA phase) was predicted, including several significant ferrimagnets, such as Ti_2MnAl, Ti_2VAs and Mn_2CoAl[6]. These compounds can possess ferrimagnetic and either half-metallic or spin gapless semi-conductive properties simultaneously. For these materials, direct observation of the ferrimagnetic ordering is a key issue to modulate the magnetic ordering. In recent reports[10], a small saturation magnetization was observed in these materials, implying a ferrimagnetic ordering. However, direct experimental evidence is lack to clarify the atomic magnetic ordering for the ferrimagnetic inverse Heusler compounds with high Curie temperature. The difficulty of clarifying the magnetic ordering of these Heusler compounds is attributed to their high Curie temperature and the similar magnetic properties between ferrimagnet and ferromagnet at low temperature. Therefore, it is necessary to investigate the element-specific magnetic moment arrangement directly at room temperature. X-ray magnetic circular dichroism (XMCD) is an unique technique to reveal the element magnetic moment arrangement directly[13-15]. The XMCD measurement provides an approach to observe element-resolved moment value and arrangement in magnetic materials directly. In last decades, a few full Heusler ferrimagnets have been investigated via XMCD measurements and the antiparallel arrangements have been observed in some of them, such as Mn_2VAl and $Mn_{2-x}Co_xVAl$[16][17]. However, for the novel ferrimagnetic inverse Heusler compounds with spin gapless semi-conductive property such as Mn_2CoAl and Ti_2MnAl, their ferrimagnetic ordering have not been confirmed yet. In this work, we investigate the element-resolved magnetic configuration of the inverse Heusler compound Mn_2CoAl epitaxial film with B2 phase via XMCD measurements. The XMCD measurements directly reveal that the spin moments of Mn are antiparallel with the spin moments of Co and the film has a very low net magnetization of ~0.34 μ_B/f.u., confirming a compensated-ferrimagnet-like ordering in the B2 phase Mn_2CoAl film.

Mn_2CoAl film with a thickness of 30 nm was grown on MgO(001) by molecular beam epitaxy at temperature of 280 °C with a based pressure of 1.5×10^{-10} mbar. Mn, Co and Al sources were evaporated by three K-cells respectively and co-deposited on the substrate. The deposition rate and the composition were calibrated by a quartz crystal oscillator. An *in-situ* reflected high energy electron diffraction (RHEED) was used to monitor the growth of the film. After the growth of Mn_2CoAl film, 3 nm Al was covered on the films to protect the film from oxidation. Then the crystalline structure and growth orientation of the film were determined using high resolution X-ray diffraction (HR-XRD) measurements by Cu Kα radiation with a wavelength of 0.154 nm. Vibrating sample magnetometer (VSM) measurements were performed to characterize the basic magnetic properties of the film. In order to investigate the atomic moment of Mn and Co atoms, the element-resolved XAS and XMCD measurements at Mn and Co $L_{2,3}$ absorption edges were performed at beamline IO10 of Diamond Light Source in the U. K. The helicity of the X-ray was switched in an external magnetic field of 3 T, which was applied perpendicularly to the surface of the film to saturate the magnetization of the film. The XAS spectra were recorded using total electron yield (TEY) with both left-helicity (σ^+) and right-helicity (σ^-) X-ray. XMCD spectra were obtained by taking the difference of the XAS spectra with σ^+ and σ^- X-ray. All the measurements were executed at room temperature.

For Heusler compounds Mn_2CoAl, it has been suggested that the inverse Heusler structure with XA phase possesses the lowest formation energy. The structure of XA phase is shown in Fig. 1(a). While epitaxially grown on MgO substrate, the Mn_2CoAl

film grows along the orientation as Mn_2CoAl (001)[110]//MgO(001)[100]. This growth orientation is demonstrated by the RHEED patterns shown in Fig. 1(b). Furthermore, the crystal structure of the Mn_2CoAl film can be determined by XRD[7]. Here, XRD out-of-plane θ-2θ scans were performed to clarify the structure and growth orientation. Fig. 1(c) shows the results of θ-2θ scans with a sample tilting angle $\chi = 0^{o}$ for the planes parallel to the substrate surface. It is obvious that the XRD data shows a clear (002) peak and a (004) peak, which confirms a well formation of B2 phase of an out-of-plane growth orientation of Mn_2CoAl(001)//MgO(001). The integral intensity ratio I(002)/I(004) also demonstrates a dominant status of B2 phase in the films. Besides, the inset of fig. 1(c) shows the result of θ-2θ scans with a sample tilting angle of 54.7^{o}, in which only (222) peaks at 54.18^{o} are found. The absence of (111) peaks at 27.09^{o} demonstrates that there is no XA phase in this film, and the film forms a B2 phase with the growth temperature of 280 ^{o}C, in which the Al and Mn(B) atoms occupy their locations randomly.

Fig. 1(d) shows the hysteresis loop of the Mn_2CoAl film at room temperature, which was obtained by VSM. In view of the in-plane anisotropy of the Mn_2CoAl films, the field is applied in plane and swept from -6000 Oe to 6000 Oe[18]. The obvious hysteresis loop demonstrates that the Mn_2CoAl film possesses a ferromagnet-like phase at room temperature, and the Curie temperature of the film is higher than room temperature. The film has a low net moment of only 0.33 μ_B/f.u., which is much smaller than the ferromagnetic Heusler compounds such as Co_2FeAl and Co_2MnSi, and is similar to the compensated ferrimagnet such as Mn_2Ru_xGa and Ti_2MnAl[8][10]. Such small magnetization hints a compensated ferrimagnetic ordering in B2 Mn_2CoAl film.

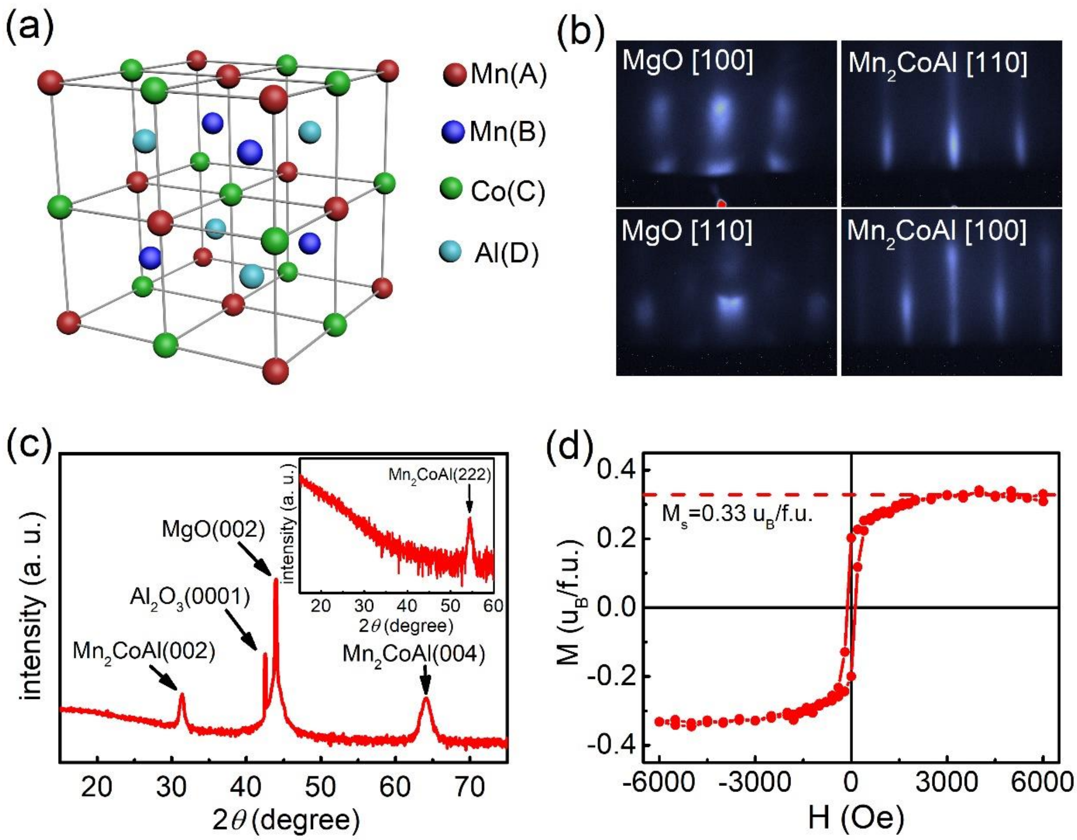

Fig. 1. The characteristic of the Mn_2CoAl film grown on MgO (001). (a) The schematic of inverse-Heusler lattice structure of XA phase Mn_2CoAl. (b) The RHEED patterns of Mn_2CoAl film and MgO substrate. The electron beam is injected following a grazing incident configuration along the [100] and [110] orientation of the MgO substrate. (c) The results of XRD θ-2θ scans with the sample tilting angle χ = 0º. The inset is the result with χ = 54.7º. The Al_2O_3(0001) peak is the peak of the sample holder of the XRD system. And the MgO(002) peak is the peak of the substrate. (d) The hysteresis loop of the Mn_2CoAl film. The external magnetic field is applied in the film plane and swept between -6000 Oe to 6000 Oe.

The XAS and XMCD spectra of the Mn_2CoAl film at Mn and Co $L_{2,3}$ absorption edges are presented in Fig. (2). XAS spectra are normalized by the photon flux. Clear metallic peaks of Mn and Co $L_{2,3}$ edges are observed, as shown in Fig 2(a) and (b), confirming that there is no oxidization at the surface of the Mn_2CoAl film. We notice that there are obvious shoulder peaks in the Mn and Co XAS spectra near the main peaks of L_3 absorption edges, as highlighted by the blue arrows in Fig. 2(a) and 2(b). These shoulder peaks have been observed in some other Heusler compounds and were attributed to the photoelectron scattering from the ordered lattice[19,20]. The shoulder peaks are also an evidence of the high ordering of Co and Mn atoms in the Mn_2CoAl film[19]. The XMCD spectra are obtained by taking the difference of the XAS spectra with left and right helical incoming X-ray, as shown in Fig. 2(c) and (d). The most arresting fact is that the XMCD peaks of Mn $L_{2,3}$ edges exhibit clear opposite sign with the Co peaks. The opposite sign of XMCD signal between Mn and Co $L_{2,3}$ peaks is an indisputable evidence that the atomic magnetic moments of Mn and Co are antiparallel with each other. It should be noted that in this work the XMCD measurements do not clearly distinguish the moment of specific Mn atoms at different sites, thus the Mn atomic moment mentioned in this report means the average atomic moment of all the Mn atoms. The XMCD spectra of the Mn in Fig. 2(c) show a splitting at the L_3 edge as highlighted by the red arrow. While the multiple splitting usually happens in oxide materials, this feature is rare in alloys despite the totally metallic XAS spectra of Mn atoms[14-17][21]. This splitting was mainly be found in some Heusler alloys which contained Mn element[16][17][19]. It suggests that there is a spin localization of Mn(A)-*d* electrons despite the delocalized character of one of the spin bands[19]. In Mn_2CoX inverse Heusler compounds, the spin localization can be attributed to Mn-Co *3d* hybridization, and is also a feature of the half-metallicity. Thus, the splitting at the Mn L_3 edge in the XMCD spectra suggests that the Mn_2CoAl with B2 phase possesses a half-metallic property.

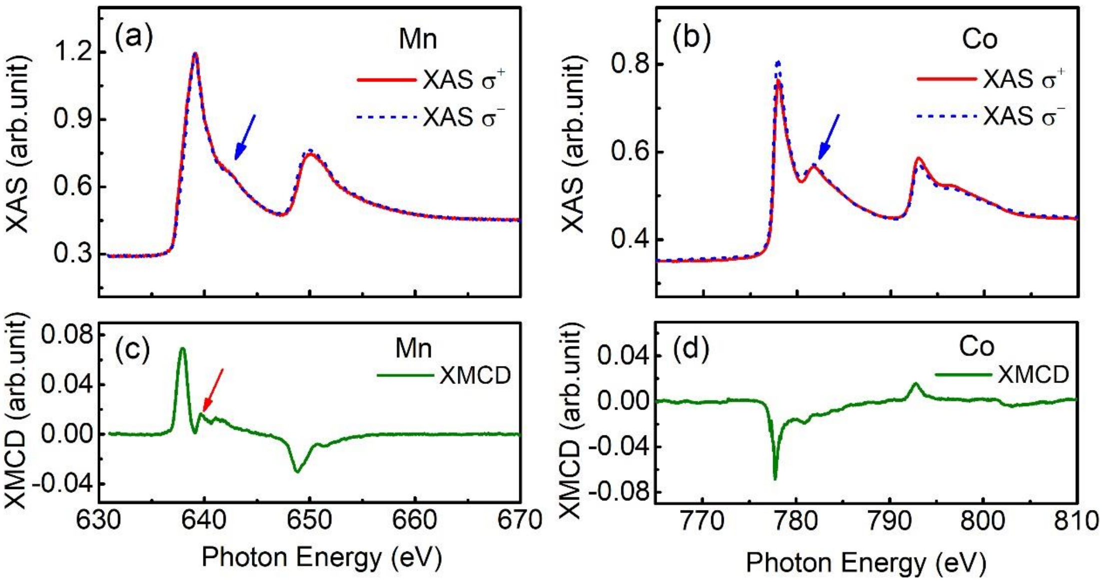

Fig. 2. XAS and XMCD spectra of Mn and Co atoms at L_2 and L_3 absorption edge. (a), (b) are the XAS spectra and (c), (d) are the XMCD spectra. The external magnetic field of 3 T is applied perpendicularly to the surface of the film to insure that the film is saturately magnetized. The blue arrows in (a) and (b) mark the shoulder peaks at the L_3 absorption edge of Mn and Co, respectively. The red arrow in (c) marks the split at Mn XMCD L_3 peak.

In order to quantify the magnitude and arrangement of the spin and orbital magnetic moments of Mn and Co atoms from the XAS and XMCD measurements, we have analyzed the spectra by using the magneto-optical sum rules. At the $L_{2,3}$ edges of Mn and Co, the electrons are promoted by the soft X-ray from *2p* core level to unoccupied *3d* states, providing an approach to directly investigate the magnetically polarized *3d* band. The spin (m_s) and orbital (m_l) moments of Mn and Co atoms are calculated according to the following equations[13][15][21]:

$$m_l = -\frac{4qn_h}{3rPcos\theta}$$

$$m_s = \frac{(4q-6p)n_h}{rPcos\theta}$$

The values of the parameters p, q, and r are obtained from the integrals of the XMCD and XAS spectra. p is the L_3 peak integral intensity in XMCD spectra, q is the sum of the $L_{2,3}$ peaks integral intensity, and r is the sum of the $L_{2,3}$ peaks integral intensity of XAS. P and θ is the circular polarization ratio of the X-ray and the angle between the incident light and the magnetization direction, respectively ($P = 1$ and $\theta = 0$ in this work). n_h is the number of $3d$ holes, and its magnitude is taken to be 4.3 for Mn and 2.5 for Co[7]. By using the sum rules, the spin moments (m_s), orbital moments (m_l) and total atomic moments (m_{tot}) of Co and Mn atoms are obtained, as shown in Table. 1. To help the discussion, we define the Mn spin moment to be the positive direction. For both Mn and Co, m_l is nearly one order of magnitude smaller than m_s, which agrees with the previous works[22]. The m_s and m_l of Mn atoms are 0.32 μ_B/f.u. and 0.03 μ_B/f.u., respectively, combined as a total atomic moment of 0.35 μ_B/f.u.. The m_s and m_l of Co are -0.27 μ_B/f.u. and -0.09 μ_B/f.u., respectively, combined as a total atomic moment of -0.36 μ_B/f.u.. From the quantitative analysis of the atomic moments, it can be further confirmed that the Co and Mn atoms conform an antiparallel arrangement in the film. The total magnetization of the Mn_2CoAl film obtained by XMCD is 0.34 μ_B/f.u., which is in accordance with the result of 0.33 μ_B/f.u. obtained by the VSM measurements.

XMCD							**VSM**
m_s(Mn) (μ_B/atom)	m_l(Mn) (μ_B/atom)	m_{tot}(Mn) (μ_B/atom)	m_s(Co) (μ_B/atom)	m_l(Co) (μ_B/atom)	m_{tot}(Co) (μ_B/atom)	m (total) (μ_B/f.u.)	m(total) (μ_B/f.u.)
0.32 (±0.03)	0.03 (±0.01)	0.35 (±0.03)	-0.27 (±0.03)	-0.09 (±0.02)	-0.36 (±0.04)	0.34 (±0.05)	0.33 (±0.03)

Table. 1. The spin moments (m_s), the orbit moments (m_l) and the total atomic moments (m_{tot}) of Mn and Co atoms in the Mn_2CoAl film. The total magnetization m obtained by XMCD and VSM is also shown in the table.

In recent theoretical reports on XA phase Mn_2CoAl, the orbit hybridization and the exchange coupling were clarified as exhibited in Fig. 3(a) and the left side of Fig. 3(b)[23-25]. As shown in Fig 3(a), $3d$ orbits of the Mn(A) and Co(C) are hybridized firstly to generate each three states for t_{2g} and t_{1u}, and each two states for e_g and e_u. Then the e_g and t_{2g} states of [Mn(A)-Co(C)] system are hybridized with Mn(B) $3d$ states[24]. This hybridization makes XA phase Mn_2CoAl to follow Slater-Pauling rule: m=Nv-24, where m is the moment per formula and Nv is the number of the valence electrons per formula[23][24]. Slate-Pauling rule indicates that XA phase Mn_2CoAl possesses a magnetization of 2 μ_B/f.u.[6]. Besides, for the exchange coupling in XA Mn_2CoAl, Mn(A)-Mn(B) (antiferromagnetic) and Co(C)-Mn(B) (ferromagnetic) nearest neighbor coupling plays a dominant role[25]. Hence, the magnetic moments of Mn(B) (2.80 μ_B/f.u.) and Co(C) (0.94 μ_B/f.u.) are parallel with each other, while the magnetic moments of Mn(B) and Mn(A) (1.65 μ_B/f.u.) are antiparallel. Because the atomic moment of Mn(B) is larger than that of Mn(A), the net moment of Mn is parallel to that of Co(C)[6].

However, our experimental results provide an alternative of the magnetic arrangement of Mn_2CoAl. In our work, an antiparallel arrangement between Mn and Co atomic moments is identified unambiguously by the XMCD spectra. The atomic moments are also smaller than the theoretical prediction. These two factors make the net magnetization of Mn_2CoAl with B2 phase similar to that of the compensated ferrimagnet. This compensated-ferrimagnetic-like phase should be related to the detailed crystal structures of the film. The XRD results in Fig. 1(c) confirm the formation of B2 ordering, suggesting a highly ordered Mn(A)-Co(C) arrangement and a mixture of the Mn(B) and Al atoms in the lattice of the Mn_2CoAl film[7]. The mixture of the Mn(B) and Al atoms can disturb the [Mn(A)-Co(C)]-Mn(B) orbit hybridization and the Mn(A)-Mn(B), Co(C)-Mn(B) nearest neighbor exchange coupling as shown in the right side of Fig. 3(b). The antiparallel arrangement between Mn(A) and Co(C) moments can be maintained, because the exchange couplings of Mn(A)-Mn(B), Mn(B)-Mn(C) and Mn(A)-Co(C) keep them to be antiparallel[25]. But the status of Mn(B) and the magnitude of all the atomic moments may be changed due to the disturbing of the orbit hybridization and exchange coupling caused by the mixture of Mn(B) and Al. Thus, a compensated-ferrimagnetic-like property can be observed in B2 phase Mn_2CoAl. However, in this work the XMCD measurements do not visually distinguish the moment distribution of Mn atoms across different sites. Further studies are needed to clarify the arrangement of Mn atomic moments in B2 phase Mn_2CoAl.

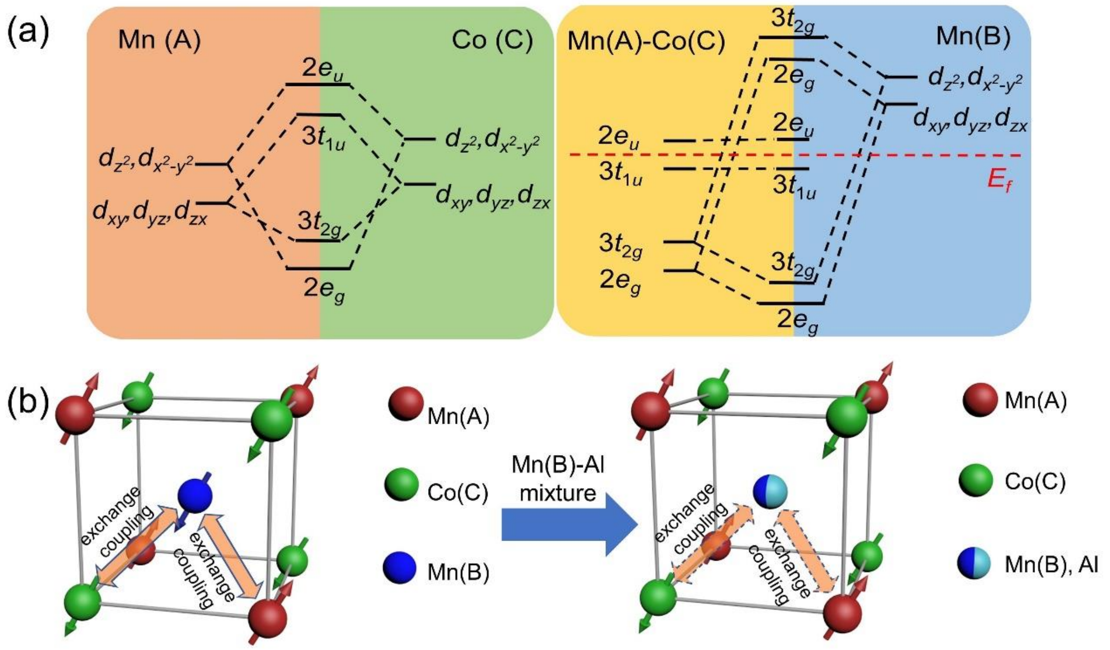

Fig. 3 (a) The sketch of hybridizations between the d-orbitals of atoms at different sites in XA phase Mn_2CoAl for spin down electrons. The hybridization for spin up electrons is identical to that for spin-down electrons only with different relative energy. The red dot line E_f represent the location of Fermi level. (b) the atomic moment arrangement and the major exchange coupling in XA phase Mn_2CoAl (left) and B2 phase Mn_2CoAl (right). The red, blue and green arrows at each atom site mean the atomic moment relative direction of Mn(A), Mn(B) and Co(C) atoms, respectively. And the orange double-end arrows mark the major exchange coupling.

In summary, we have revealed a compensated ferrimagnetic ordering in inverse Heusler compound B2 Mn_2CoAl epitaxial film via XMCD measurements. It is verified that the atomic moments of Mn are antiparallel with that of Co by the opposite sign of the Mn and Co XMCD peaks at L_2 and L_3 edge. A splitting is observed at the Mn L_3 edge XMCD peak and suggests a Mn(A)-Co *3d* orbit hybridization in Mn_2CoAl Heusler alloys. The atomic magnetic moment of Mn and Co are quantitively obtained via magneto-optical sum rules, further confirming an antiparallel arrangement between Mn and Co atomic moment. The low net magnetization of only 0.34 μ_B/f.u. conforms with the compensated ferrimagnetic materials. This work spreads the potential applications of inverse Heusler compound Mn_2CoAl in spintronics as a compensated ferrimagnetic half metal, which can provide high spin polarization, low magnetization and low stray field simultaneously. It also suggests a possibility to construct a totally compensated ferrimagnetic state in B2 phase Mn_2CoAl by component modulation.

Acknowledgement

The authors thank Prof. Haihu Wen, Prof. Huan Yang and Mr. Jin Si for the assistant of magnetic property characterization, and thank Prof. Yuefeng Nie and Mr. Heng Zhang for the assistant of XRD measurements. This work is supported by National Key Research and Development Program of China (Grant No. 2016YFA0300803), the National Natural Science Foundation of China (Grant No. 61427812, 11774160), the Natural Science Foundation of Jiangsu Province of China (No. BK20192006), the Fundamental Research Funds for the Central Universities (Grant No. 021014380113), National Science and Technology Major Project (2017ZX01032101-001), UK EPSRC (EP/S010246/1), Royal Society (IEC\NSFC\181680), and Leverhulme Trust (LTSRF1819\15\12). Diamond Light Source is acknowledged to beamline I10 under proposal MM22532.

Data available on request from the authors.

Reference:

[1] R. A. de Groot, F. M. Mueller, P. G. van Engen, and K. H. J. Buschow, Phys. Rev. Lett. **50**, 2024 (1983).

[2] J.-H. Park, E. Vescovo, H.-J. Kim, C. Kwon, R. Ramesh and T. Venkatesan, Nature **392**, 6678 (1998).

[3] S. A. Wolf, D. D. Awschalom, R. A. Buhrman, J. M. Daughton, S. von Molnár, M. L. Roukes, A. Y. Chtchelkanova, and D. M. Treger, Science 294, 5546 (2001).

[4] M. I. Katsnelson, V. Yu. Irkhin, L. Chioncel, A. I. Lichtenstein, and R. A. de Groot, Rev. Mod. Phys. **80**, 315 (2008).

[5] S. Ouardi, G. H. Fecher, C. Felser, and J. Kübler, Phys. Rev. Lett. **110**, 100401 (2013).

[6] S. Skaftouros, K. Özdoğan, E. Şaşıoğlu, and I. Galanakis, Appl. Phys. Lett. **102**, 022402 (2013).

[7] L. Bainsla, R. Yilgin, J. Okabayashi, A. Ono, K. Suzuki, and S. Mizukami, Phys. Rev. B. **96**, 094404 (2017).

[8] H. Kurt, K. Rode, P. Stamenov, M. Venkatesan, Y.-C. Lau, E. Fonda, and J. M. D. Coey, Phys. Rev. Lett. **112**, 027201 (2014).

[9] A. K. Nayak, M. Nicklas, S. Chadov, P. Khuntia, C. Shekhar, A. Kalache, M. Baenitz, Y. Skourski, V. K. Guduru, A. Puri, U. Zeitler, J. M. D. Coey and C. Felser, Nat. Mat. **14**, 679 (2015).

[10] Wuwei Feng, Xiao Fu, Caihua Wan, Zhonghui Yuan, Xiufeng Han, Nguyen Van Quang, and Sunglae Cho, Phys. Status Solidi RRL **9**, 641-645 (2015).

[11] P. Lukashev, P. Kharel, S. Gilbert, B. Staten, N. Hurley, R. Fuglsby, Y. Huh, S. Valloppilly, W. Zhang, K. Yang, R. Skomski, and D. J. Sellmyer, Appl. Phys. Lett. **108**, 141901 (2016).

[12] J. Han and G. Gao, Appl. Phys. Lett. **113**, 102402 (2018).

[13] C. T. Chen, Y. U. Idzerda, H.-J. Lin, N. V. Smith, G. Meigs, E. Chaban, G. H. Ho, E. Pellegrin, and F. Sette, Phys. Rev. Lett. **75(1)**, 152 (1995).

[14] S. Banerjee, W. L. O'Brien, and B. P. Tonner, J. Mag. Mag. Mat. **198**, 267-269 (1999).

[15] J. S. Claydon S. Hassan, C. D. Damsgaard, J. B. Hansen, C. S. Jacobsen, Y. B. Xu, G. van der Laan, J. Appl. Phys. **101**, 09J506 (2007).

[16] T. Kubota, K. Kodama, T. Nakamura, Y. Sakuraba, M. Oogane, K. Takanashi, and Y. Ando, Appl. Phys. Lett. **95**(22), 222503 (2009).

[17] M. Meinert, J. M. Schmalhorst, G. Reiss, and E. Arenholz, J. Phys. D: Appl. Phys. **44(21)**, 215003 (2011).

[18] G. Z. Xu, Y. Du, X. M. Zhang, H. G. Zhang, E. K. Liu, W. H. Wang, and G. H. Wu, Appl. Phys. Lett. **104**, 242408 (2014).

[19] N. D. Telling, P. S. Keatley, G. van der Laan, R. J. Hicken, E. Arenholz, Y. Sakuraba, M. Oogane, Y. Ando, and T. Miyazaki, Phys. Rev. B **74**, 224439 (2006).

[20] H. J. Elmers, G. H. Fecher, D. Valdaitsev, S. A. Nepijko, A. Gloskovskii, G. Jakob, G. Schönhense, S. Wurmehl, T. Block, C. Felser, P.-C. Hsu, W.-L. Tsai, and S. Cramm, Phys. Rev. B **67**, 104412 (2003).

[21] S. Seong, E. Lee, H. Y. Kim, Y. Kim, J. Baik, J. -S. Kang, Curr. Appl. Phys. **18**, 1190–1195 (2018).

[22] M. E. Jamer, B. A. Assaf, G. E. Sterbinsky, D. A. Arena, and D. Heiman, J. Appl. Phys. **116**, 213914 (2014).

[23] S. Trudel, O. Gaier, J. Hamrle, and B Hillebrands, J. Phys. D: Appl. Phys. **43**, 193001 (2010).

[24] G. Z. Xu, E. Liu, Y. Du, G. X. Li, G. D. Liu, W. H. Wang, G. H. Wu, EPL **102**, 17007 (2013).

[25] M. Meinert, JM. Schmalhorst, and G Reiss, J. Phys.: Condens. Matter. **23**, 116005 (2011).

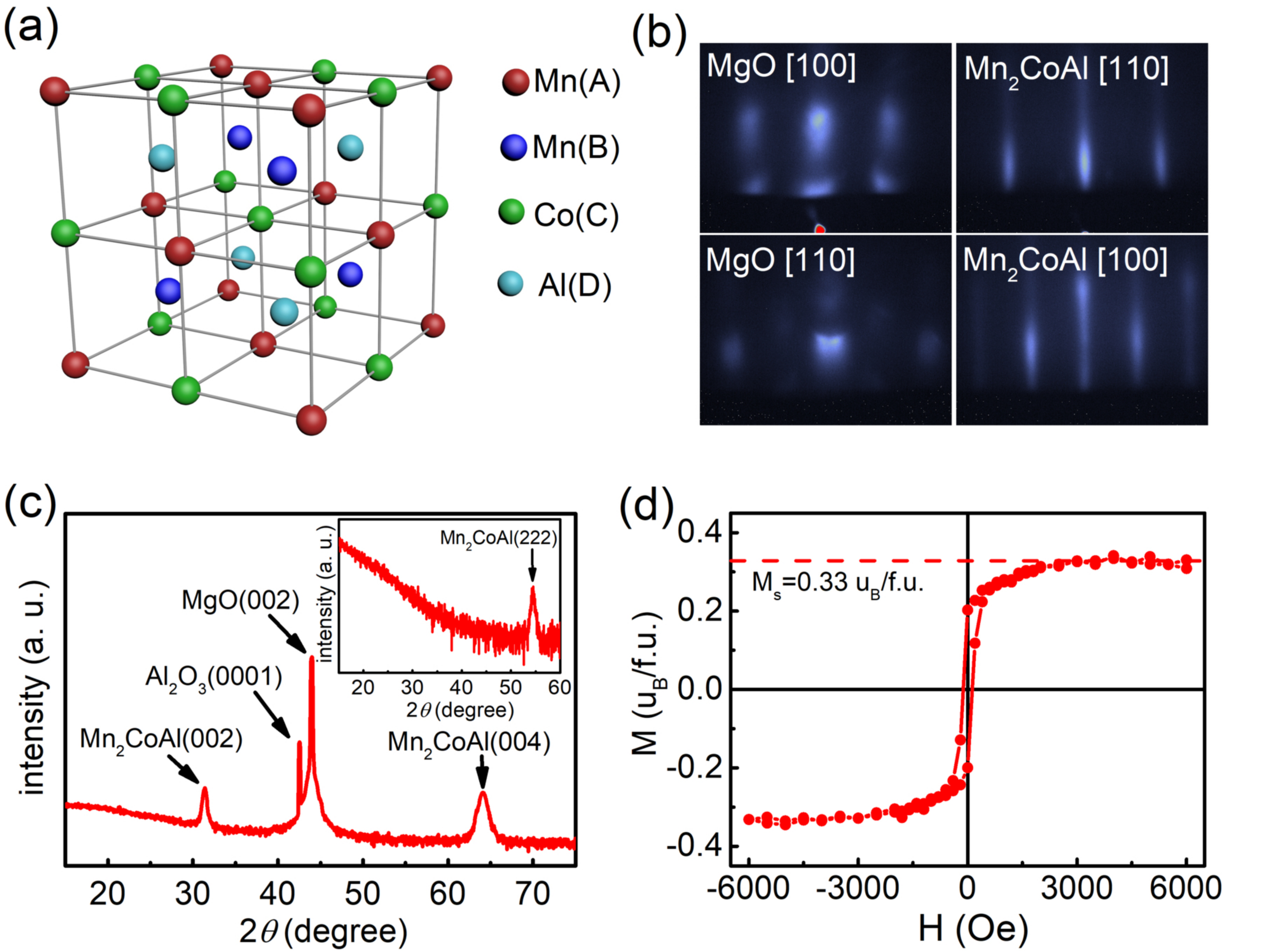
(a)
Mn(A)
Mn(B)
Co(C)
Al(D)
(b)
MgO [100]
Mn$_2$CoAl [110]
MgO [110]
Mn$_2$CoAl [100]
(c)
intensity (a. u.)
MgO(002)
Al$_2$O$_3$(0001)
Mn$_2$CoAl(002)
Mn$_2$CoAl(004)
Mn$_2$CoAl(222)
intensity (a. u.)
20 30 40 50 60
2θ (degree)
20 30 40 50 60 70
2θ (degree)
(d)
M (u$_B$/f.u.)
M$_s$=0.33 u$_B$/f.u.
0.4 0.2 0.0 -0.2 -0.4
-6000 -3000 0 3000 6000
H (Oe)

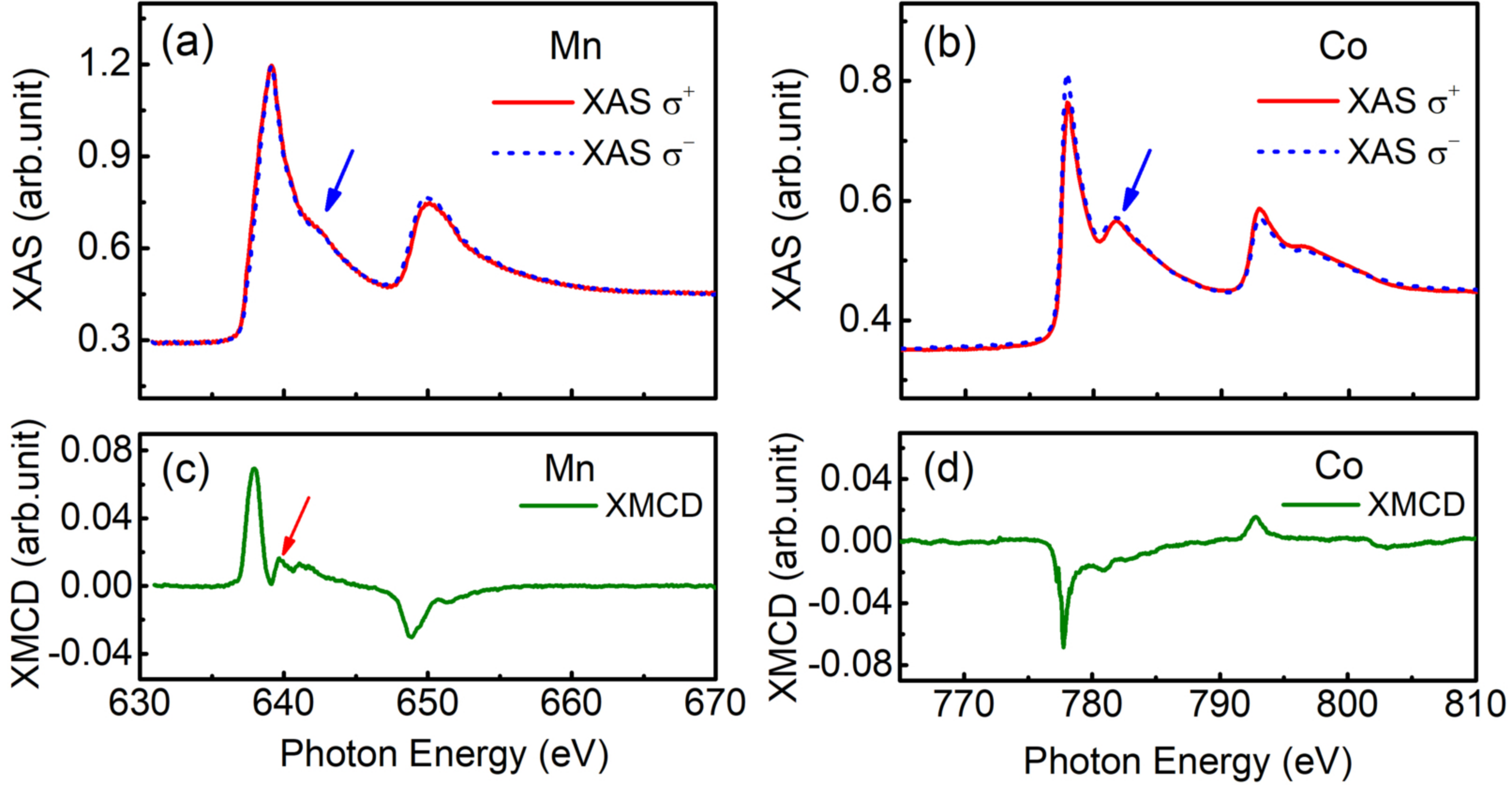
(a)
Mn
XAS σ+
XAS σ−
XAS (arb.unit)
1.2
0.9
0.6
0.3
(b)
Co
XAS σ+
XAS σ−
XAS (arb.unit)
0.8
0.6
0.4
(c)
Mn
XMCD
XMCD (arb.unit)
0.08
0.04
0.00
-0.04
630
640
650
660
670
Photon Energy (eV)
(d)
Co
XMCD
XMCD (arb.unit)
0.04
0.00
-0.04
-0.08
770
780
790
800
810
Photon Energy (eV)

(a)
Mn (A)
Co (C)
2e_u
3t_{1u}
3t_{2g}
2e_g
$d_{z^2}, d_{x^2-y^2}$
d_{xy}, d_{yz}, d_{zx}
Mn(A)-Co(C)
Mn(B)
3t_{2g}
2e_g
2e_u
3t_{1u}
E_f
(b)
exchange coupling
exchange coupling
Mn(A)
Co(C)
Mn(B)
Mn(B)-Al mixture
Mn(B), Al